Glucose Metabolism and AMPK Signaling Regulate Dopaminergic Cell Death Induced by Gene (α-Synuclein)-Environment (Paraquat) Interactions

Annadurai Anandhan [1,2] · Shulei Lei [3] · Roman Levytskyy [4] ·
Aglaia Pappa [5] · Mihalis I. Panayiotidis [6] · Ronald L. Cerny [3] ·
Oleh Khalimonchuk [4] · Robert Powers [3] · Rodrigo Franco [1,2]

Abstract While environmental exposures are not the single cause of Parkinson's disease (PD), their interaction with genetic alterations is thought to contribute to neuronal dopaminergic degeneration. However, the mechanisms involved in dopaminergic cell death induced by gene-environment interactions remain unclear. In this work, we have revealed for the first time the role of central carbon metabolism and metabolic dysfunction in dopaminergic cell death induced by the paraquat (PQ)-α-synuclein interaction. The toxicity of PQ in dopaminergic N27 cells was significantly reduced by glucose deprivation, inhibition of hexokinase with 2-deoxy-D-glucose (2-DG), or equimolar substitution of glucose with galactose, which evidenced the contribution of glucose metabolism to PQ-induced cell death. PQ also stimulated an increase in glucose uptake, and in the levels of glucose transporter type 4 (GLUT4) and Na$^+$-glucose transporters isoform 1 (SGLT1) proteins, but only inhibition of GLUT-like transport with STF-31 or ascorbic acid reduced PQ-induced cell death. Importantly, while autophagy protein 5 (ATG5)/unc-51 like autophagy activating kinase 1 (ULK1)-dependent autophagy protected against PQ toxicity, the inhibitory effect of glucose deprivation on cell death progression was largely independent of autophagy or mammalian target of rapamycin (mTOR) signaling. PQ selectively induced metabolomic alterations and adenosine monophosphate-activated protein kinase (AMPK) activation in the midbrain and striatum of mice chronically treated with PQ. Inhibition of AMPK signaling led to metabolic dysfunction and an enhanced sensitivity of dopaminergic cells to PQ. In addition, activation of AMPK by PQ was prevented by inhibition of the inducible nitric oxide syntase (iNOS) with 1400W, but PQ had no effect on iNOS levels. Overexpression of wild type or A53T mutant α-synuclein stimulated glucose accumulation and PQ toxicity, and this toxic synergism was reduced by inhibition of glucose metabolism/transport and the pentose phosphate pathway (6-aminonicotinamide). These results demonstrate that glucose metabolism and AMPK regulate dopaminergic cell death induced by gene (α-synuclein)-environment (PQ) interactions.

✉ Robert Powers
  rpowers3@unl.edu

✉ Rodrigo Franco
  rfrancocruz2@unl.edu

1 Redox Biology Center, University of Nebraska-Lincoln, N200 Beadle Center, Lincoln, NE 68588-0662, USA

2 School of Veterinary Medicine and Biomedical Sciences, University of Nebraska-Lincoln, Lincoln, NE 68583-0905, USA

3 Department of Chemistry, University of Nebraska-Lincoln, Hamilton Hall, Lincoln, NE 68588-0304, USA

4 Department of Biochemistry, University of Nebraska-Lincoln, Lincoln, NE 68588-0662, USA

5 Department of Molecular Biology and Genetics, Democritus University of Thrace, University Campus, Dragana, 68100 Alexandroupolis, Greece

6 School of Life Sciences, Heriot-Watt University, Edinburgh, EH14 4AS Scotland, UK

Published online: 20 June 2016

Springer

Introduction

Aging, genetic alterations, and environmental factors contribute to the etiology of Parkinson's disease (PD) [1, 2]. Mutations in genes such as α-synuclein (SNCA) account for only 10 % of PD occurrences [3]. SNCA missense mutations (A30P, A53T, and E46K) cause autosomal dominant PD [4]. Genomic multiplications are also linked to familial PD, where the age of onset and severity of the disease correlate with SNCA copy number [5]. SNCA duplications have been reported in sporadic PD patients as well [6–8]. Importantly, whether SNCA alterations are found or not, the presence of fibrillar cytoplasmic misfolded aggregates and intermediates in multiple brain regions is considered one of the pathological hallmarks of PD [5]. Exposure to environmental toxicants including pesticides (e.g., paraquat [PQ] and rotenone) is recognized as an important PD risk factor [9]. The redox cycling pesticide PQ is used to study the susceptibility of dopaminergic cells to increase reactive oxygen species (ROS) formation [10, 11]. Importantly, the toxicity of PQ in dopaminergic cells is modulated by PD-related genes. For example, in culture cells, PQ-induced cell death is enhanced by the (over)expression of wild type (WT) or the Ala53Thr (A53T) mutant α-synuclein [12]. Transgenic mice overexpressing the A53T mutant show an increased sensitivity to the combination of PQ and the fungicide maneb [13], and to neonatal exposure to iron and PQ [14]. However, the mechanisms by which PQ and α-synuclein interact to induce dopaminergic cell loss are still unclear.

Energy failure and oxidative stress associated with mitochondrial dysfunction are hallmarks of PD. A disruption of the electron transport chain (ETC), the tricarboxylic acid (TCA or Krebs) cycle, and oxidative phosphorylation (OXPHOS) has been found in PD brains [15, 16]. However, while energy dysfunction and oxidative stress are recognized as major contributors to the pathogenesis of PD [17], the role of alterations in central carbon metabolism is poorly understood. Glucose is the obligatory energy substrate of the adult brain. A decrease in glucose metabolism and abnormally elevated lactate levels have been reported in PD patients [18–20], while an increase in lactate levels has also been reported to promote α-synuclein accumulation [21]. Glucose metabolism in neurons is primarily directed to the generation of reducing equivalents via the pentose phosphate pathway (PPP) to support antioxidant defenses [22]. In addition, downregulation of PPP enzymes and failure to increase the antioxidant reserve are early events in the pathogenesis of sporadic PD [23]. Alterations in cellular energy are tightly monitored by the adenosine monophosphate-activated protein kinase (AMPK), a master regulator of metabolism [24]. Contradicting results have been reported regarding the role of AMPK in dopaminergic cell death [21, 25–29]. AMPK regulates a myriad of processes involved in the cellular response to energy deficiency. Thus, understanding the role of AMPK signaling in dopaminergic cell death requires a more in-depth characterization of the processes regulated downstream of its activation. We have recently demonstrated that alterations in central carbon metabolism (glucose) and upregulation of the PPP contribute to the toxicity of PQ [30]. These findings have prompted our interest in determining the role of central carbon metabolism in gene-environment interactions involved in dopaminergic cell death.

Materials and Methods

Cell Culture and Reagents The immortalized (SV40) rat dopaminergic mesencephalic cell line N27 was kindly provided by Dr. Michele L. Block (Indiana University School of Medicine). N27 cells were grown in Roswell Park Memorial Institute (RPMI) medium 1640 (Hyclone) supplemented with 10 % fetal bovine serum (FBS, Atlanta Biologicals), penicillin (200 U/ml)-streptomycin (200 μg/ml) (Hyclone), and 2 mM L-glutamine (Hyclone), and maintained at 37 °C in 5 % CO_2 humidified atmosphere. N27 cells express key features of dopaminergic neurons such as neuron-specific enolase, nestin, tyrosine hydroxylase, and dopamine transporter (DAT), and contain homovanillic acid and dopamine [31]. Wild type (WT), α1 or α2 knockout (KO, −/−) or double KO AMPK (DKO-AMPK$^{-/-}$), and ULK1 KO (ULK1$^{-/-}$) mouse embryonic fibroblasts (MEFs) were kindly provided by Dr. Mondira Kundu (St. Jude Children's Research Hospital) and Dr. Benoit Viollet (Institut Cochin INSERM) [32]. MEFs were cultured in Dulbecco's Modified Eagle Medium: Nutrient Mixture F-12 (DMEM/F-12, Hyclone) media supplemented with 10 % FBS, penicillin (200 units/ml)-streptomycin (200 μg/ml), 2 mM L-glutamine, and 200 μM β-mercaptoethanol (Thermo Fisher Scientific). Phase contrast images of cells were taken using a Zeiss ×20/0.3 LD-A-Plan Ph1 objective and a Moticam 580 (5.0 MP) camera. Chloroquine and 1-methyl-4-phenylpyridinium iodide (MPP$^+$) were obtained from Sigma-Aldrich. PQ, 2-deoxy-d-glucose (2-DG), and ascorbic acid (AA) were from Acros Organics. 5-Aminoimidazole-4-carboxamide ribonucleotide (AICAR) and torin 1 were from Cayman Chemical. N-[[3-(aminomethyl)phenyl]methyl]-ethanimidamide dihydrochloride (1400W) was from AdipoGen. STF-31 (4-[[[[4-(1,1-dimethylethyl)phenyl]sulfonyl]amino]methyl]-N-3-pyridinylbenzamide) was from Tocris Bioscience. Rapamycin was purchased from LC laboratories. 6-Aminonicotinamide (6-AN) was obtained from Alfa Aesar. Compound C (CC) was obtained from Enzo Life Sciences, and phlorizin from Selleckchem. Torin 1, rapamycin, STF-31, phlorizin, CC, and 1400W were dissolved in DMSO. Control conditions included the appropriate vehicle, which never exceed >0.01 % (v/v).

Recombinant Adenoviral Vectors Replication-deficient recombinant adenoviruses (Ad5CMV) encoding wild type (WT) or mutant A53T α-synuclein were kindly provided by Dr. Jean-Christophe Rochet (Purdue University) [33]. The adenovirus encoding dominant-negative K130R mutant ATG5 was generously provided by Dr Gökhan S. Hotamisligil (Harvard School of Public Health) [34]. Ad5CMV-MnSOD, Ad5CMV-CuZnSOD, Ad5CMV-catalase, and Ad5CMV-mito-catalase (mitochondria-targeted catalase, with a MnSOD mitochondrial signal peptide) were provided by Dr. Matthew C. Zimmerman (University of Nebraska Medical Center) [35]. The adenovirus encoding human dominant-negative HA-tagged AMPKα1 with a D159A mutation in the ATP binding domain was purchased from Eton Bioscience. The AMPKα1 mutant lacks the capacity to bind ATP and competes with WT AMPKα1 for binding with the β and γ subunits [36]. Adenovirus containing only the CMV promoter (Ad-Empty) or encoding green fluorescent protein (Ad-GFP) were used as controls. Adenoviruses were amplified and tittered as described previously [37, 38]. Cells were infected with adenoviral vectors at the indicated multiplicity of infection (MOI) for 24 h, washed, and subsequently treated under the specified experimental conditions.

Cell Death Determination (Loss of Plasma Membrane Integrity and Glutathione depletion) Loss of cell viability was determined using flow cytometry by measuring propidium iodide uptake (PI, 1 μg/ml) (Life Technologies) as a marker for plasma membrane integrity loss. Changes in intracellular glutathione (GSH) levels were simultaneously determined using monochlorobimane (mBCl, 10 μM) (Molecular Probes). Flow cytometry was performed as described previously [10, 30, 39, 40].

Protein Extraction, Electrophoresis, and Western Immunoblot SDS-PAGE electrophoresis and western immunoblotting (WB) were performed as explained before [40]. Blots were blocked and incubated with the corresponding antibodies as recommended by the manufacturers. Antibodies against phosphorylated (p)-AMPK1α (Thr 172, #2535), p-ACC (Ser 79, #11818), AMPKα2 (#2757), α-synuclein (carboxy-terminal sequence, #2642), p-mTOR (Ser 2448, #5536), and p-ULK1 (Ser 555, #5869; Ser 317, #6887; Ser 757, #6888) were from Cell Signaling; AMPKα1 (Ab32047), mTOR (Ab32028), and ULK1 (Ab65050) were obtained from Abcam; and LC3B (L7543) was from Sigma-Aldrich. When indicated, blots were probed with β-actin (A2228, Sigma-Aldrich) to verify equal protein loading. Relative densitometry analysis of WBs was done using the ImageJ Program (National Institutes of Health, http://rsb.info.nih.gov/ij).

Immunostaining of Glucose Transporters Cells were harvested and washed with phosphate-buffered saline (PBS), then fixed in 4 % paraformaldehyde (PFA) at room temperature (RT) in the dark. Cells were centrifuged and washed with staining buffer (PBS, 1 % FBS, 0.1 % (w/v) NaN₃, pH 7.4). Cells were stained for 1 h with antibodies recognizing the N-terminal extracellular domain of the glucose transporter type 4 (GLUT4) (sc1606, Santa Cruz) or antibodies that recognize amino acids 402-420 in the cytoplasmic region of SGLT1 (07-1417 EMD Millipore). Samples were washed and subsequently stained with secondary anti-goat Alexa fluor 647 or anti-rabbit Alexa fluor 488 (Molecular Probes) antibodies for GLUT4 or SGLT-1 detection, respectively. Following incubation, cells were washed with the staining buffer and analyzed with a 488-nm laser and the emission was detected through a 530/30 emission filter in a FACSort (BD Biosciences/Cytek-DxP-10 upgrade) flow cytometer.

Glucose Transport After treatment, cells were incubated with 50 μM 2-[N-(7-nitrobenz-2-oxa-1,3-diazol-4-yl)amino]-2-de-oxy-D-glucose (2-NBDG, Cayman Chemical), a fluorescent analogue of 2-DG, for 1 h prior to analysis by flow cytometry. Subsequently, cells were harvested, washed, and 2-NBDG fluorescence was analyzed by flow cytometry (488 nm ex, 530/30 em).

In Vivo Mouse Model of PQ Toxicity C57BL/6J mice (8–10 weeks old) (Jackson Labs) were chronically treated with PQ as explained before [41]. Animals were analyzed 1 week after the last injection. Mice were decapitated and the brain regions were removed for WB analysis or metabolomics. All procedures involving animals were reviewed and approved by the Institutional Animal Care and Use Committee of the University of Nebraska-Lincoln (Project 1025) following NIH guidelines.

Metabolic Phenotyping Oxygen consumption (OCR, pmol/min) or extracellular acidification rates (ECAR, mpH/min) were determined using XF^e24 Analyzer (Seahorse Biosciences). After treatment, cells were incubated for 1 h in HCO₃/4-(2-hydroxyethyl)-1-piperazineethanesulfonic acid (HEPES) free medium prior to OCR and ECAR measurements. Measurements were normalized to total protein concentration. ECAR was used as an indirect measurement of glycolysis. Changes in the pH of media sensitive to glycolysis inhibitors (2-DG, 5 mM) are considered to be predominately originated from the excretion of lactic acid (lactate and H⁺) after its conversion from pyruvate [42]. The glycolytic reserve capacity was evaluated by changes in ECAR in the presence of oligomycin (1 μM), which inhibits ATP synthase in the ETC. OCR was used as an indicator of mitochondrial function [43].

Metabolomics Data Collection and Analysis After treatment, cells were washed to remove the remaining media, and metabolites were extracted as previously described [30].

Mouse brain tissues were extracted and immediately frozen in liquid N_2. Tissues were homogenized using Lysing Matrix D and Fastprep-24 (MP Biomedicals) in 50 % methanol/ddH$_2$O followed by centrifugation. Metabolites were re-extracted once by the same solvent, combined, and normalized to net wet weight. The combined extracts were split for one-dimensional (1D) ^{1}H nuclear magnetic resonance (NMR) and mass spectrometry (MS) analysis. For 2D ^{1}H-^{13}C Heteronuclear Single-Quantum Correlation (HSQC) experiment, ^{12}C-glucose in the medium was replaced with ^{13}C-glucose (3.5 g/l) and 500 μM TMSP was used for chemical shift referencing and normalization. The 1D ^{1}H and 2D ^{1}H-^{13}C HSQC spectra were collected on a Bruker Avance III-HD700-MHz spectrometer equipped with a quadruple resonance QCI-P cryoprobe (^{1}H, ^{13}C, ^{15}N, ^{31}P) and a SampleJet automated sample changer, and analyzed as previously described [30, 44].

Metabolome extracts for MS analysis were diluted with 50 % methanol/ddH$_2$O for positive mode detection or 50 % NH$_4$ acetate/ddH$_2$O for negative mode detection. Twenty micromolar or 50 μM reserpine was used as an internal standard. Direct-infusion electrospray ionization MS (DI-ESI-MS) in both positive and negative mode was performed on a Synapt G2 HDMS quadrupole time-of-flight instrument (Waters Corp.). The detailed operation conditions and spectra processing parameters have been described previously [30].

As described previously, metabolites were identified from NMR and MS spectral data by comparing experimental ^{1}H and ^{13}C chemical shifts, and m/z values to reference values in several online metabolomics databases [30]. Error tolerances of 0.08 and 0.25 ppm were used for ^{1}H and ^{13}C chemical shifts, respectively. A 20-ppm error tolerance was used for m/z values. The intensities of all the NMR peaks assigned to a metabolite were used to report an average peak intensity (concentration) change between treatment classes.

Statistical Analyses Experimental replicas were independent and performed on separate days. Collected data were analyzed by using one-way or two-way ANOVA, and the appropriate post hoc test using the SIGMA-PLOT/STAT package. When ANOVA assumptions were not met (normality [Shapiro–Wilk test] or equal variance), Kruskal-Wallis one-way ANOVA on Ranks or data transformation (two-way ANOVA) was performed on the collected data. Data were plotted as mean ± standard error (SE) using the same package for statistical analysis. Flow cytometry plots and immunoblots presented show the results of representative experiments. Multivariate analysis of the metabolomics datasets was obtained using a multiblock (MB) structure and principal component analysis (PCA) and partial least square projections to latent structures (PLS) modeling functions in our MVAPACK software suite (http://bionmr.unl.edu/mvapack.php) [45]. The NMR spectra were preprocessed in MVAPACK as previously described [30, 46]. Mahalanobis distance derived p values, 95 % confidence ellipses, and dendrograms from MB-PLS-DA models were generated using our PCA/Partial Least Squares-Discriminant Analysis (PLS-DA) utilities (http://bionmr.unl.edu/pca-utils.php) implemented in MVAPACK [47, 48]. The MB-PLS-DA models were validated using CV-ANOVA [49] sevenfold Monte Carlo single cross-validation [50]. P values <0.05 were considered as a statistically significant difference between comparisons.

Results

Glucose Metabolism Regulates PQ-Induced Dopaminergic Cell Death Independent of Autophagy

The rat dopaminergic mesencephalic cell line N27 was exposed to PQ in the presence or absence of glucose. Glucose deprivation significantly reduced PQ-induced cell death (Fig. 1a, b). Cells grown on medium supplemented with galactose and glutamine are more sensitive to mitochondrial toxins or defects [51], as galactose slows glucose metabolism, forcing cells to rely on glutaminolysis and OXPHOS phosphorylation for ATP production [52]. Figure 1c demonstrates that N27 cells cultured in glucose-deficient or galactose-supplemented medium are more sensitive to the mitochondrial complex I inhibitor MPP$^+$. In contrast, galactose exerted a protective effect against PQ toxicity (Fig. 1b). An inhibition of glycolysis and a reduction in the glycolytic capacity of N27 cells, determined by changes in the extracellular medium acidification (ECAR), were observed when cells were grown in glucose-free or galactose-supplemented media (Fig. 1d, e), demonstrating that the protective effects of glucose deprivation and galactose supplementation are related to inhibition of glucose metabolism. Co-treatment of N27 cells with the hexokinase inhibitor 2-DG also inhibited PQ-induced cell death (Fig. 1f). These results demonstrate that glucose metabolism contributes to PQ-induced cell death.

Inhibition of glucose metabolism induces autophagy [32]. Thus, a role for autophagy in the protective effects of glucose deprivation against PQ toxicity is expected. Autophagy flux was evaluated by determining the levels of the autophagosomal marker LC3-II in the presence of CQ, an inhibitor of the acid-dependent breakdown of autolysosome cargo. Separately, glucose deprivation and PQ increased autophagy flux, but together a decrease in the basal levels of LC3-I or
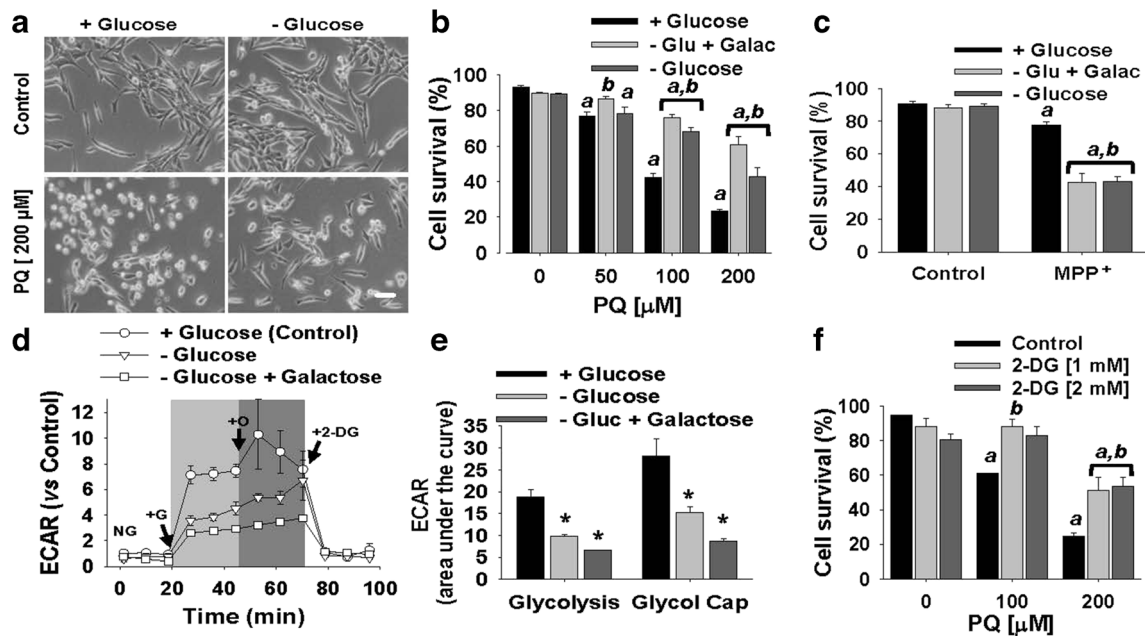
Fig. 1 Inhibition of glucose metabolism protects against PQ toxicity independent of autophagy. Rat dopaminergic N27 cells were grown in culture media with or without glucose, or in glucose-free medium supplemented with galactose. When indicated, cells were treated with PQ or MPP⁺ (2.5 mM) for 48 h in the presence or absence of 2-DG. **a** Phase contrast images of representative experiments. *Scale white bar* = 50 μm. Cell survival (**b**, **c** and **e**, **f**) was determined by the simultaneous analysis of plasma membrane integrity (PI uptake) and intracellular GSH content (mBCl fluorescence). Bar graphs represent percents of viable cells (cell survival) and data are means ± SE of at least $n = 3$ independent experiments. In **d**, **e**, glycolysis rates (*gray region* in **d**) and glycolytic reserve capacity of cells (*dark gray region* in **d**) were evaluated by changes in the ECAR sensitive to 2-DG. Glycolysis is observed as an increase in ECAR when switching cells from a glucose-free environment (NG) to a medium containing 10 mM glucose (+G). Glycolytic reserve capacity is determined by addition of oligomycin (+O). Bar graphs in **e** represent the area under the curve of data in **d**. Data in **d** and **e** are means ± SE of at least $n = 3$ independent experiments and are represented with respect to control (+ glucose). Two-way ANOVA Holm-Sidak *post hoc* test: *a*, $p < 0.05$ vs no PQ or MPP⁺ within the corresponding category of ±glucose, galactose, or 2-DG; *b* $p < 0.05$, vs +glucose (**b**, **c**) or vs control (**f**), within the corresponding toxicant treatment. *t* test: *$p < 0.05$, vs +glucose

LC3-II was observed (Supplementary Fig. 1a). ATG5 is essential for autophagosome formation [53]. We and others have demonstrated that overexpression of a dominant-negative form (dn) of ATG5 is an efficient approach to inhibit autophagy [34]. dnATG5 inhibited autophagy (*data not shown*) and increased the sensitivity of cells to PQ, but only induced a slight decrease in the protective effect of glucose deprivation (Supplementary Fig. 1b).

The AMPK/mammalian target of rapamycin (mTOR)/unc-51 like autophagy activating kinase 1 (ULK1 or ATG1) signaling axis regulates autophagy induced by glucose deprivation. mTOR complex 1 (mTORC1) activation inhibits lysosome biogenesis and autophagy [54]. Phosphorylation of mTOR (pmTOR) at Ser 2448 correlates with mTOR activity [55]. We observed that PQ induced a dose-dependent increase in pmTOR (Supplementary Fig. 1c). To further determine the effect of pharmacological modulation of autophagy on PQ-induced cell death, we used the mTORC inhibitors rapamycin (mTORC1) and torin 1 (mTORC1 and mTORC2). While rapamycin decreased pmTOR (Supplementary Fig. 1d) and increased autophagy flux

(CQ data in Supplementary Fig. 1e), it did not counteract the inhibition of autophagy found in PQ-treated cells (CQ data in Supplementary Fig. 1e). Furthermore, neither rapamycin nor torin 1 had an effect on PQ-induced cell death (Supplementary Fig. 1f, g).

ULK1 is essential for autophagy induction [56]. Upon glucose deprivation, AMPK promotes autophagy by activating ULK1 through the phosphorylation of Ser 317, Ser 777 [32], or Ser 555 [57], while under nutrient adequacy mTOR inhibits autophagy by phosphorylation of ULK1 at Ser 757 disrupting its interaction with AMPK [32]. PQ was shown to induce a dose-dependent increase in ULK1 Ser 555 and a decrease in Ser 757 phosphorylation, while low PQ doses only induced an increase in pULK1 Ser 317 (Supplementary Fig. 1c). ULK1 KO MEFs were observed to be more sensitive to PQ (Supplementary Fig. 1h). These results demonstrate that while ATG5/ULK1-dependent autophagy exerts a protective effect against PQ-induced cell death, pharmacological inhibition of mTOR signaling has no effect on cell death progression. Our findings also demonstrate that the protective effects of reduced glucose metabolism against PQ toxicity are largely independent from the induction of autophagy.

PQ Induces an Increase in Glucose Uptake and in the levels of Glucose Transporters

Glucose uptake was evaluated with the fluorescent analogue 2-NBDG. PQ treatment was observed to induce an increase in 2-NBDG uptake (Fig. 2a). Glucose is transported across the plasma membrane by a saturable transport system involving the Na$^+$-independent glucose transporters (GLUT), and the Na$^+$-dependent glucose transporters (SGLT). We observed that treatment with PQ induced an increase in the levels of SGLT1 and GLUT4 transporters (Fig. 2b, c). Interestingly, inhibition of GLUT-like glucose transport with STF-31 significantly reduced PQ-induced cell death (Fig. 2d), while phlorizin, an inhibitor of SGLT1, had only a slight effect on cell death progression (Fig. 2e). AA is structurally similar to glucose and acts as a competitive inhibitor of glucose transport [58]. AA also decreased the toxicity of PQ (Fig. 2f). These results demonstrate that glucose transport stimulated by PQ contributes to dopaminergic cell death.

Selective Metabolic Dysfunction and AMPK Activation in the Midbrain and Striatum of Mouse Chronically Treated with PQ

Using an integrated (NMR/MS) metabolomics approach [30], we evaluated PQ-induced metabolic dysfunction in C57Bl/6J mice chronically treated with PQ. Changes in the metabolome were found to be primarily restricted to the midbrain and striatum, but not the cortex. The three-dimensional (3D) MB-PCA score plots in Fig. 3a compare the metabolic profiles from different brain regions of control and PQ-treated mice. The corresponding p values calculated from the Mahalanobis distances between the classes is evidence that a statistically significant metabolic change was only observed for the striatum and midbrain regions after PQ treatment. The metabolites contributing to the class separation in the midbrain and striatum regions were identified from the orthogonal projections to patent structures-discriminate analysis (OPLS-DA) back-scaled loadings (Supplementary Fig. 2) and the observed percent fold changes are plotted in Fig. 3b. The fold changes were calculated by comparing the peak intensities in the original 1D
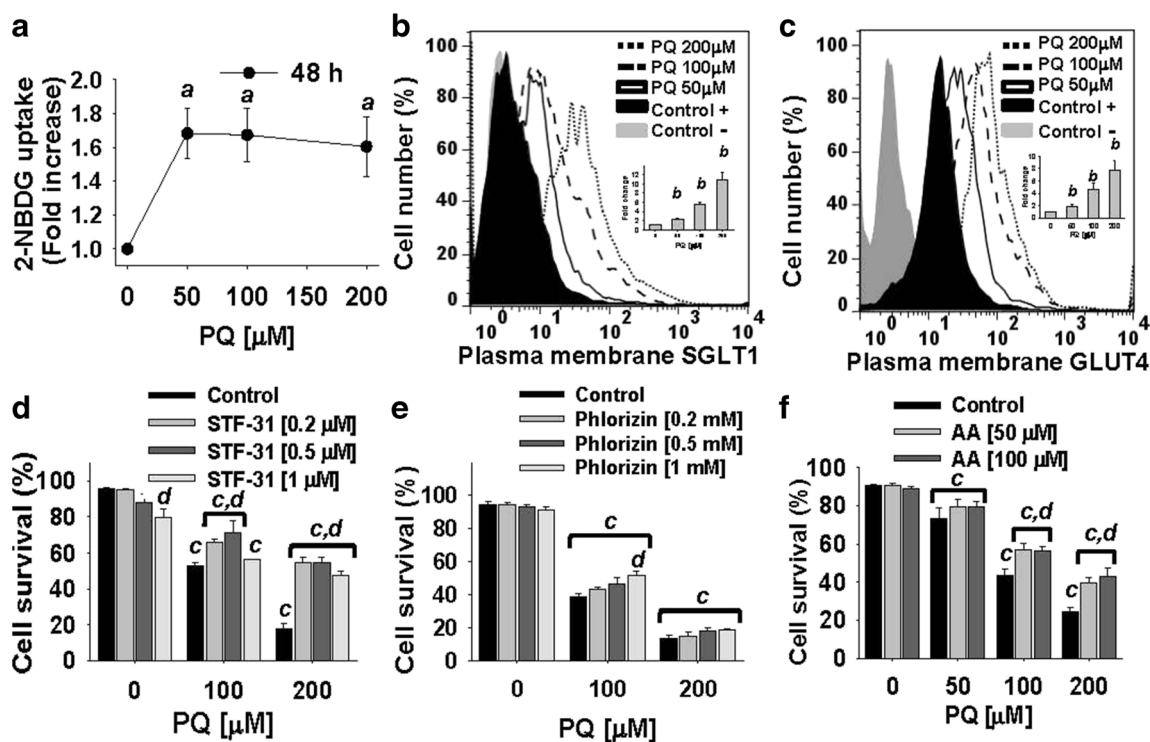
Fig. 2 PQ increases glucose transport and the translocation of glucose transporters. Cells were treated with PQ for 48 h. In **a**, glucose transport was evaluated by the uptake of 2-NBDG. In **b**, **c**, the expression levels of the glucose transporters were assessed by flow cytometry (immunofluorescence). Histograms represent changes in the mean fluorescence value for the immunostaining of SGLT1 or GLUT4. Inset bar graphs represent the fold change in mean fluorescence with respect to control (+). Negative control (−, secondary antibody only) is included for comparison. The survival of cells treated with PQ in the presence or absence of STF-31 (**d**), phlorizin (**e**), or AA (**f**) was determined as explained in Fig. 1. Bar graph represents percents of viable cells (cell survival). Data in all graphs are means ± SE of at least $n = 3$ independent experiments. One-way ANOVA Holm-Sidak *post hoc* test: *a*, $p < 0.05$ vs no PQ. ANOVA on Ranks Student-Newman-Keuls *post hoc* test: *b*, $p < 0.05$ vs control +. Two-way ANOVA Holm-Sidak *post hoc* test: *c*, $p < 0.05$ vs no PQ within the corresponding ±STF-31 or phlorizin category; *d*, $p < 0.05$ vs control (no glucose transport inhibitor) within the corresponding PQ concentration
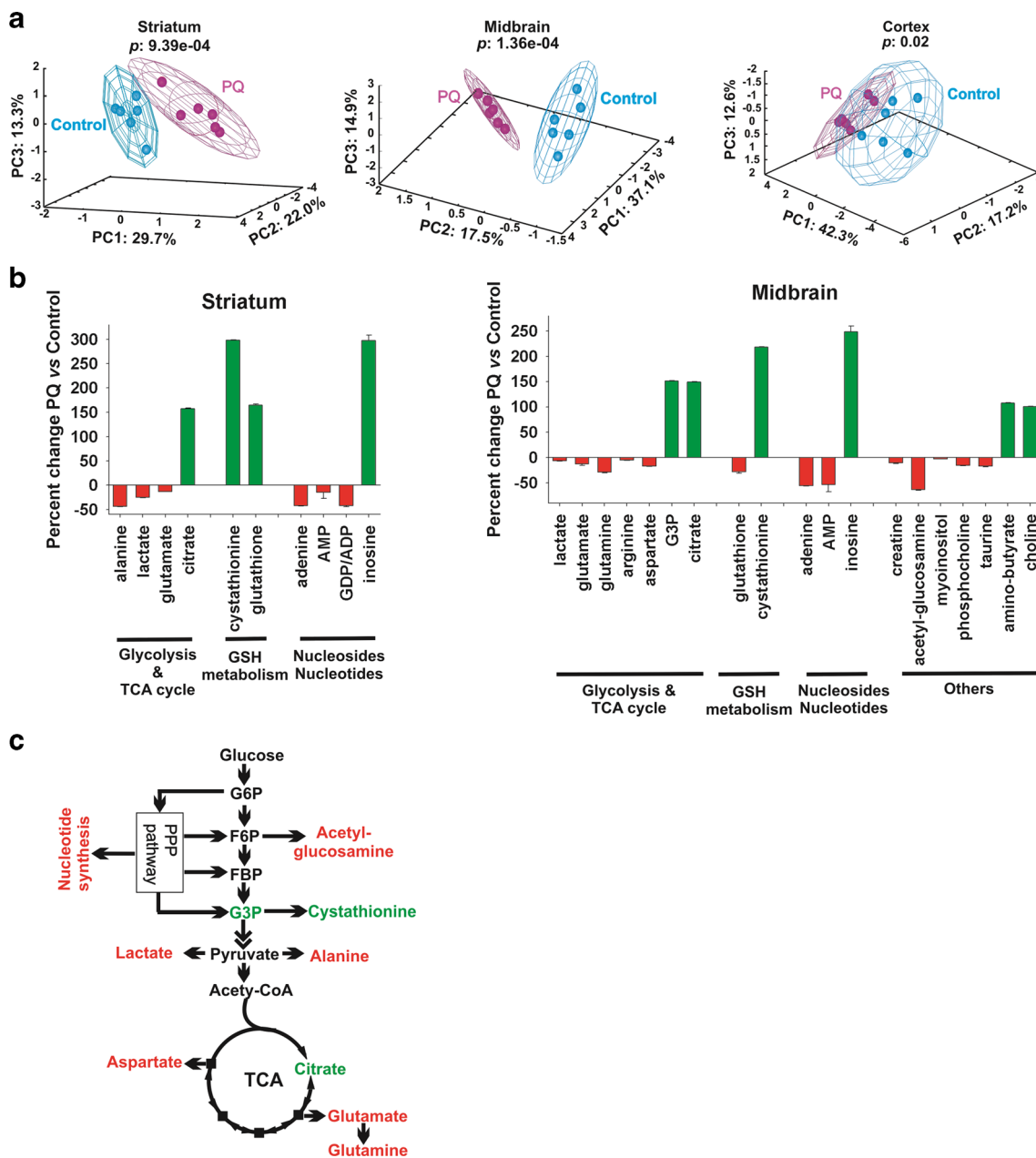
Fig. 3 Paraquat treatment induces metabolome alterations in the brain regions of midbrain and striatum. C57Bl/6J mice were exposed chronically to PQ. One week after the final injection of PQ or PBS, animals were euthanized to isolate metabolites from the midbrain, striatum, and cortex regions. Integrated positive and negative-ion DI-ESI-MS and 1D ^{1}H NMR was used to characterize the alterations in the metabolic profiles of midbrain, striatum, and cortex regions from control and PQ-treated mice. In **a**, metabolomics profiles are represented in 3D MB-PCA scores plots. The p values in the MB-PCA scores plots indicate the significance of metabolome changes after PQ treatment, with $p < 0.05$ values considered significant ($n = 6$). The ellipsoids correspond to the 95 % confidence limits from a normal distribution for each cluster. In **b**, the percent fold change for metabolites contributing to class separation in **a** as identified from OPLS-DA back-scaled loadings plots (Supplemental Fig. 2) are plotted. The percent fold changes are all significant ($p < 0.05$) based on a paired t test. The *green colored bars* indicate metabolites with a fold-increase after PQ treatment, whereas *red colored bars* indicate a metabolite decreased after PQ treatment. In **c**, a simplified metabolic network is shown that summarizes metabolite alterations (from **b**) within glucose metabolism (e.g., glycolysis and the TCA cycle) after PQ treatment. Metabolites colored red decreased after PQ treatment, while metabolites colored green increased after PQ treatment.. *G6P*, glucose 6-phosphate; *F6P* fructose 6-phosphate; *FBP* fructose 1,6-biphosphate; *G3P* glyceraldehyde 3-phosphate

^{1}H spectral data between controls and PQ treatments. Metabolites within glycolysis (evidenced by changes in lactate and alanine) and the TCA cycle (glutamate) were significantly decreased in mice treated with PQ. PQ also induced an accumulation of citrate, which is ascribed to its inactivating effect on aconitase (Fig. 3b) [30, 59]. The diagram in Fig. 3c summarizes the metabolites within glucose metabolism significantly changed after PQ treatment (e.g., glycolysis and TCA

cycle), corroborating our previous in vitro findings that PQ impairs glycolysis (observed as a decrease in lactate and alanine content) [30], while increasing the levels of citrate due to the inactivation of aconitase [59]. Alterations in cellular metabolism are sensed by AMPK [24]. Interestingly, an increase in pAMPK and its substrate pACC (acetyl-CoA carboxylase) levels were also observed in the midbrain and striatum regions, but not in the cerebellum or cortex of PQ-treated mice (Fig. 4a). These results corroborate our previous in vitro studies [30] that demonstrated PQ alters glucose metabolism, and further reveal that the midbrain and striatum metabolome are more sensitive to a chronic PQ treatment.

AMPK Signaling Protects Against Dopaminergic Cell Death Induced by PQ

PQ was observed to induce a dose-dependent increase in pAMPK in N27 cells (Fig. 4b). Interestingly, we only observed an increase in pACC at low PQ concentrations (≤ 100 μM), suggesting that while PQ increases pAMPK, AMPK activity is impaired at toxic concentrations of PQ (≥ 100 μM) (Fig. 4b). Overexpression of a dominant-negative form of AMPKα1 decreased pACC induced by PQ treatment (Fig. 4c) and stimulated PQ-induced cell death (Fig. 4d). Contradictory results were observed when using pharmacological modulators of AMPK activity. AICAR, an AMP analogue capable of enhancing AMPK activity, augmented PQ toxicity in N27 cells (Supplementary Fig. 3a). CC, a pyrrazolopyrimidine derivative that inhibits AMPK, had no effect on cell death progression (Supplementary Fig. 3b). Nevertheless, recent studies have questioned the specificity of AICAR and CC, in which a wide variety of non-specific effects have been reported [60]. Thus, our results obtained using dnAMPK overexpression seem more reliable and consistent with expectations from AMPK inactivation.

Glucose deprivation and galactose supplementation inhibited glucose metabolism and PQ-induced cell death (Fig. 1). Interestingly, the increased sensitivity to PQ toxicity induced by dnAMPK was associated with impaired glycolysis and glycolytic capacity (Fig. 4e). However, overexpression of dnAMPK also inhibited OCR/ECAR ratios (Fig. 4f) demonstrating that inhibition of AMPK signaling impairs both glycolysis and mitochondrial respiration. Furthermore, the decrease in OCR/ECAR ratio induced by PQ was exacerbated by inhibition of AMPK signaling (Fig. 4f). Together, these observations demonstrate that the increase in PQ toxicity induced by inhibition of AMPK signaling is linked to metabolic dysfunction.

We further evaluated if the protective effects of glucose deprivation against PQ toxicity are linked to AMPK signaling. We observed that glucose deprivation or its substitution with galactose had no major effects on pAMPK in the presence or absence of PQ (Fig. 4g and Supplementary Fig. 3c), which may be related to the length of exposure to glucose

deprivation that is reported to increase pAMPK within a time frame <8–12 h [61]. However, both glucose and galactose increased pACC suggesting an overall increase in AMPK activity regardless of an increase of pAMPK levels (Fig. 4g and Supplementary Fig. 3c). Overexpression of dnAMPK significantly reduced the protective effects of glucose deprivation against PQ-induced cell death (Fig. 4h). We also observed that N27 cells express very low levels of the catalytic α2 subunit, which are increased upon PQ exposure (Supplementary Fig. 3d). Compensatory effects for AMPK subunits α1 and 2 have been previously reported [62]. α1, but not α2, KO ($-/-$) MEFs had an increased susceptibility to PQ toxicity (Supplementary Fig. 3e–f). However, double KO (DKO) of α1 and α2 additively enhanced PQ-induced cell death (Supplementary Fig. 3e, g). In DKO cells, the protective effect of glucose deprivation against PQ toxicity was completely abolished (Supplementary Fig. 3h). These results demonstrate that the protective effects of glucose-free conditions against PQ are linked to the activation of AMPK.

PQ-Induced AMPK Activation Is Mediated by the Inducible Nitric Oxide Synthase

Oxidative stress has been proposed to induce the activation of AMPK by either changes in the nucleotide pool or by direct oxidation of AMPK [63, 64]. Overexpression of catalase, CuZn superoxide dismutase (SOD), MnSOD, or mitochondria-targeted catalase (mito-catalase) did not prevent the increase in pAMPK induced by PQ (Fig. 5a, b and Supplementary Fig. 4a–c). PQ-induced toxicity has also been suggested to involve either the generation of nitric oxide (NO·) or the uncoupling of NO· synthase (NOS) to generate $O_2^{\cdot-}$ [65, 66]. PQ-induced AMPK activation and cell death were reduced by inhibition of the inducible NOS (iNOS) with 1400W (Fig. 5c, d). No major additive protective effects were observed when combining both glucose deprivation and 1400W (Fig. 5d). These results suggest that PQ-induced AMPK activation is mediated by iNOS.

Overexpression of α-Synuclein Potentiates the Metabolic Dysfunction, AMPK Activation, and Dopaminergic Cell Death Induced by PQ

Overexpression of WT or A53T α-synuclein for 72 h had no effect on high molecular weight aggregate formation (Fig. 6a) or cell viability (Fig. 6b and Supplementary Fig. 5a, b). However, when cells overexpressing WT or A53T α-synuclein were exposed to PQ, a synergistic toxicity was observed (Fig. 6b and Supplementary Fig. 5a, b). Importantly, the enhancement in PQ toxicity was selective for α-synuclein since it was not mimicked by overexpression of GFP (Supplementary Fig. 5c).

Fig. 4 AMPK signaling protects against PQ toxicity. In **a**, C57Bl/6J mice were exposed chronically to PQ. Mice were subsequently euthanized to isolate the midbrain, striatum, cerebellum, and cortex regions. N27 dopaminergic cells were treated with the indicated concentrations of PQ for 48 h (except for experiments in **e**, **f** where cells were treated with 25 μM PQ for 12 h). When indicated, cells were transduced with adenoviral particles encoding a dnAMPKα1 (1 MOI, unless otherwise indicated) 24 h prior to PQ treatment (**c**), or treated with PQ in media ± glucose with or without galactose supplementation. Adenoviruses containing only the CMV promoter (*Empty*) were used as control. Changes in the levels of phosphorylated (p) AMPKα1 and its substrate ACC (**a–c** and **g**) induced by PQ were evaluated by WB. *Numbers in italics* represent the relative densitometry quantification of pAMPKα1 or pACC normalized to total AMPKα1 or β-actin, respectively, and expressed with respect to control (*underlined*). Bar graphs in **a** and **c** represent the densitometry analysis of the corresponding WBs from three independent replicas. Data are represented as fold change vs the indicated control (dotted line). In **d** and **h**, the effect of the overexpression of dnAMPKα1 on PQ-induced cell death in media ± glucose was evaluated as explained in Fig. 1. Data in graphs represent percentage of viable cells (cell survival) and data are means ± SE of at least $n = 3$ independent experiments. In **e**, glycolysis rates (*gray region*) and glycolytic reserve capacity (*dark gray region*) were determined as explained in Fig. 1d. In **f**, basal OCR and ECAR rates were determined after 1 h of incubation of cells with fresh medium. Data in **e**, **f** represent means ± SE of at least $n = 3$ independent experiments. Two-way ANOVA Holm-Sidak *post hoc* test: a, $p < 0.05$ vs no PQ within the corresponding category of Empty or dnAMPKα1; b, $p < 0.05$, dnAMPKα1 vs Empty within the corresponding concentration of PQ. Two-way ANOVA Holm-Sidak *post hoc* test for ± dnAMPKα1 ± glucose data for each PQ concentration: c, $p < 0.05$, dnAMPKα1 vs Empty, within the corresponding category of ±glucose; d, $p < 0.05$, vs +glucose, within the corresponding category of Empty or dnAMPKα1

◀ **Fig. 5** AMPK activation by PQ is mediated by iNOS. N27 cells were treated with PQ for 48 h. When indicated, cells were transduced with adenoviral particles (1.5 MOI) encoding catalase (**a**) or CuZnSOD (**b**) for 24 h prior to PQ treatment, or treated in the presence of the iNOS inhibitor 1400W. Adenoviral vectors containing only the CMV promoter (*Empty*) were used as control. In **c**, cells were treated with PQ in the presence or absence of 1400W (100 μM) (**c**). Changes in the levels of phosphorylated (p) AMPKα1 (**a–c**), catalase (**a**), or CuZnSOD (**b**) were evaluated by WB. *Numbers in italics* represent the relative densitometry quantification of pAMPKα1 normalized to total AMPK α1 and expressed with respect to control (*underlined*). Bar graph in **c** represents the densitometry analysis from three independent replicas. Data are represented as fold change. Two-way ANOVA Holm-Sidak *post hoc* test: *a*, $p < 0.05$ vs no PQ within the corresponding category of ±1400W; *b*, $p < 0.05$, vs −1400W within the corresponding concentration of PQ. In **d**, the effect of 1400W on PQ-induced cell death in media ± glucose was evaluated as explained in Fig. 1. Data in graphs represent percentage of viable cells (cell survival) and data are means ± SE of at least $n = 3$ independent experiments. Two-way ANOVA Holm-Sidak *post hoc* test for ±1400W ± glucose data for each PQ concentration: *c*, $p < 0.05$, −glucose vs +glucose, within the corresponding category of ±1400W; *d*, $p < 0.05$, vs −1400W, within the corresponding category of ±glucose

We next determined the alterations in central carbon metabolism induced by PQ and the associated effect of α-synuclein overexpression. We first looked at changes in the overall metabolome of cells using an integrated NMR/MS metabolomics approach. 3D MB-PCA plots show that exposure of cells to non-toxic PQ concentrations (25 μM), or overexpression of α-synuclein, induced a significant change in the metabolome of N27 cells (Fig. 6c, d and Supplementary Fig. 5d). We observed no significant difference between the metabolome of cells overexpressing either WT or A53T α-synuclein (Supplementary Fig. 5d). Overexpression of either WT or A53T α-synuclein and exposure of cells to PQ elicited the most significant change in the metabolome as evidenced by the separation between control + PQ and WT or A53T α-synuclein + PQ experimental groups. This is corroborated by the p values listed in the associated dendrograms and matrix table generated from the MB-PCA scores plot (Fig. 6d and Supplementary Fig. 5d). Again, no significant difference was observed when comparing the metabolomes of cells overexpressing WT or A53T α-synuclein after treatment with PQ (Supplementary Fig. 5d). To identify the exact alterations in glucose metabolism induced by PQ and α-synuclein, we performed a metabolomics analysis using 2D ^{1}H–^{13}C HSQC NMR with ^{13}C-glucose as a substrate. Overexpression of α-synuclein and exposure of cells to non-toxic PQ concentrations (25 μM) enhanced glucose accumulation suggesting an impairment in glucose flux (Fig. 6e). Similar to the effect elicited by inhibition of AMPK signaling (Fig. 4e, f), overexpression of α-synuclein impaired both glycolysis and reduced the glycolytic capacity of N27 cells as well as mitochondrial respiration (OCR/ECAR ratio) (Fig. 6f, g). These results suggest that α-synuclein impairs glucose metabolism. α-Synuclein overexpression also stimulated the activation of AMPK induced by PQ (Fig. 6h and
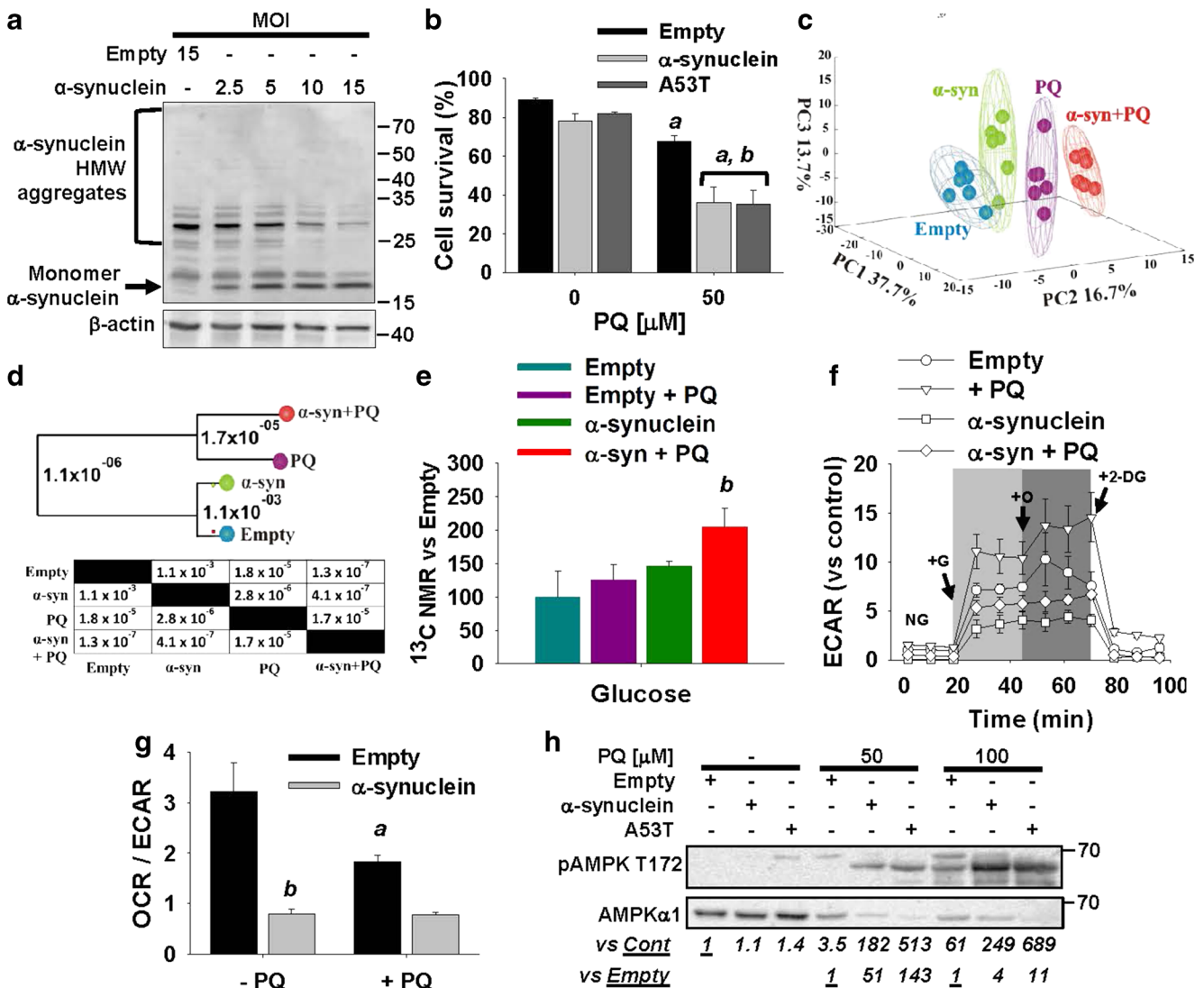
Fig. 6 α-Synuclein potentiates the metabolic dysfunction, AMPK activation, and toxicity induced by PQ. N27 dopaminergic cells were transduced for 24 h with Empty adenoviruses or adenoviruses encoding either WT or mutant A53T α-synuclein (6 MOI). In **a**, WB analysis of the levels of α-synuclein protein monomers and high molecular weight (HMW) aggregates evaluated 48 h after transduction. In **b**, cell survival after exposure to PQ for 48 h was determined as explained in Fig. 1. Bar graph represents percentage of viable cells (cell survival) and data are means ± SE of at least $n = 3$ independent experiments. In **c–e**, cells were treated with 25 μM PQ for 24 h. Metabolites were extracted for NMR/MS metabolomics. 3D MB-PCA scores plot shows the changes in the metabolome based on distances between groups (**c**). The statistical significance of the Mahalanobis distance between groups within the MB-PCA scores plot (i.e., differences in the metabolome) is illustrated by the p values in the table and the corresponding dendrogram (**d**). The ellipsoids correspond to the 95 % confidence limits from a normal distribution for each cluster. Six independent samples of metabolic extract were used for the MB-PCA multivariate analysis. In **e**, 2D ^{1}H–^{13}C HSQC NMR spectra from ^{13}C glucose labeling experiments were used to evaluate the intracellular metabolic changes shown by the MB-PCA multivariate analysis. Data represent the mean of three independent replicates. In **f, g**, cells were treated with 25 μM PQ for 12 h. In **f**, glycolysis rates (*gray region*) and glycolytic reserve capacity (*dark gray region*) were determined as explained in Fig. 1d. In **g**, basal OCR and ECAR rates were determined as explained in Fig. 4f. Data in **f, g** represent means ± SE of at least $n = 3$ independent experiments. Two-way ANOVA Holm-Sidak *post hoc* test: *a*, $p < 0.05$ vs no PQ within the corresponding ± Empty or α-synuclein category; *b*, $p < 0.05$ vs Empty within the corresponding PQ concentration. In **h**, changes in the levels of phosphorylated AMPKα1 (pAMPKα1) in cells exposed to PQ for 48 h were evaluated by WB. *Numbers in italics* represent the relative densitometry quantification of pAMPKα1 normalized to total AMPKα1, and expressed with respect to control (*underlined*)

Supplementary Fig. 5e). These results reveal that the stimulation of PQ toxicity induced by inhibition of AMPK signaling or overexpression of α-synuclein is mediated by metabolic dysfunction (i.e., an impairment of both glycolysis and mitochondrial respiration required to meet energy demands).

Finally, we determined whether glucose metabolism contributes to the synergistic toxicity between PQ and α-synuclein overexpression. Accordingly, glucose deprivation (Fig. 7a and Supplementary Fig. 5f), inhibition of glucose transport with STF-31 (Fig. 7b), and inhibition of the PPP
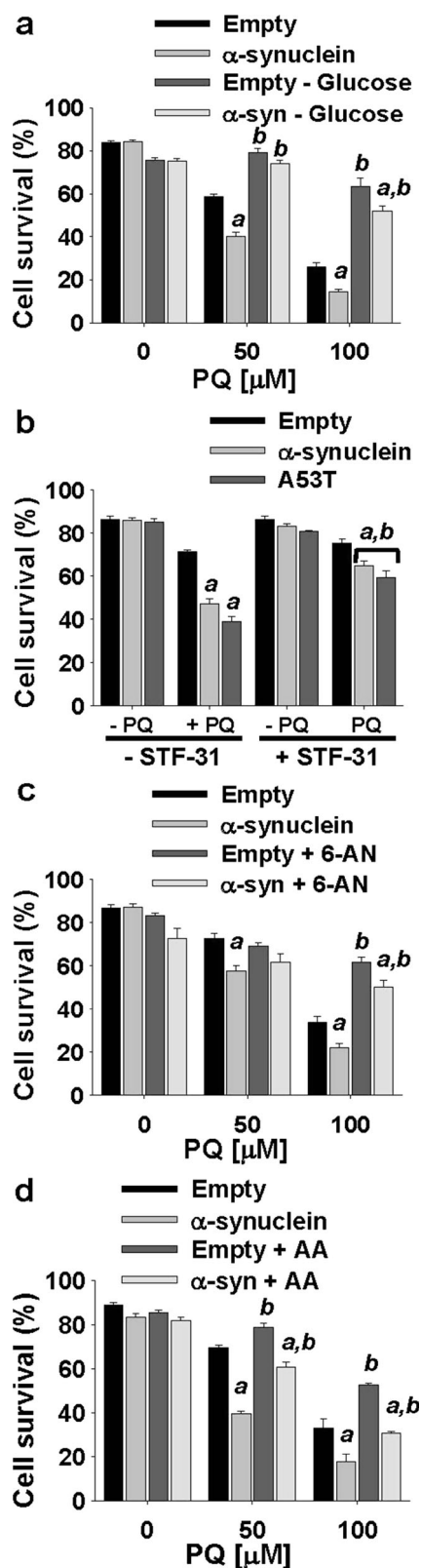
◀ **Fig. 7** Glucose metabolism and the PPP regulate the toxic synergism of α-synuclein and PQ. N27 dopaminergic cells were transduced for 24 h with Empty viral particles or adenoviruses encoding either WT or mutant A53T α-synuclein (6 MOI). After transduction, cells were treated with PQ (50 μM in **b**) for 48 h in the presence or absence of glucose (**a**), STF-31 (**b**, 0.5 μM), 6-AN (**c**, 1 mM), or AA (**d**, 100 μM). Cell survival was determined as explained in Fig. 1. Bar graphs represent percents of viable cells (cell survival) and data are means ± S.E.M. of at least $n = 3$ independent experiments. Two-way ANOVA Holm-Sidak *post hoc* test was done for each PQ concentration independently: *a, $p < 0.05$*, vs Empty, within the corresponding category of ±glucose (**a**), ±STF31 (**b**), ±6-AN (**c**), or ±AA (**d**); *b, $p < 0.05$*, vs +glucose (**a**), −STF-31 (**b**), −6-AN (**c**), or −AA (**d**), within the corresponding category of Empty or α-synuclein

environment interaction was significantly reduced by AA (Fig. 7d and Supplementary Fig. 5h). These results demonstrate that the toxic synergism of PQ and α-synuclein overexpression (gene-environment interaction) involves alterations in glucose metabolism and signaling.

It is important to note that no significant difference was observed between the effect of overexpressing WT and A53T α-synuclein on PQ-induced metabolic changes or cell death (Fig. 6b and Supplementary Fig. 5d), which suggests that the synergistic toxicity induced by A53T overexpression is only related to the overexpression of α-synuclein, but not to its mutation. Interestingly, protein sequence alignment of rat (N27 cells are rat-derived cells), mouse, and human α-synuclein showed that Thr instead of Ala is already in place at position 53 in both mouse and rat α-synuclein (Supplementary Fig. 6), which might explain the lack of difference between the synergistic toxicity induced by WT and the A53T mutant.

Overall, our results demonstrate that glucose metabolism and AMPK regulate dopaminergic cell death induced by PQ and by its toxic interaction with α-synuclein. Importantly, α-synuclein and inhibition of AMPK signaling potentiate PQ toxicity by impairing energy metabolism (glycolysis and mitochondrial respiration).

Discussion

In this work, we demonstrate that glucose metabolism and AMPK signaling regulate PQ toxicity and the synergism between PQ and α-synuclein. More specifically, we have demonstrated that PQ-induced dopaminergic cell death is directly linked to glucose metabolism and that the metabolic master regulator AMPK exerts a protective effect against PQ toxicity. Interestingly, PQ exposure induced changes in the cellular metabolome and an increased activation of AMPK, which were restricted to the midbrain and striatum regions of mice chronically treated with PQ. Furthermore, we also reported that while autophagy protects against PQ, the protective effect of glucose deprivation is largely independent of autophagy. Finally, we also demonstrated that the toxic gene-environment interaction involving α-synuclein and PQ is linked to metabolic dysfunction

using 6-AN (Fig. 7c and Supplementary Fig. 5g) abolished the stimulatory effect of either WT or A53T α-synuclein overexpression on PQ toxicity. Similarly, this toxic gene-
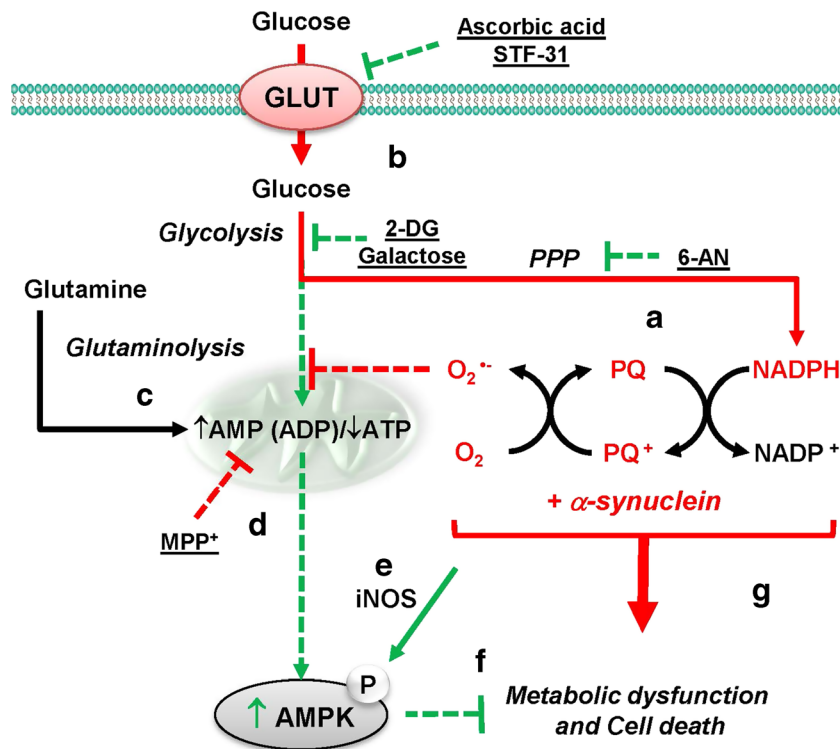
Fig. 8 Glucose metabolism and AMPK signaling regulate the toxicity of PQ + α-synuclein. We have previously demonstrated that PQ hijacks the PPP to use NADPH electrons to redox cycle and induce cell death (*a*). In this work, we have now revealed that glucose metabolism/transport contributes to PQ-induced dopaminergic cell death as evidenced by the protective effects of STF-31, AA (GLUT-like transport inhibitors), and 2-DG (glucose metabolism inhibitor) (*b*). Furthermore, we present evidence that stimulation of glutamine metabolism via the TCA cycle by galactose supplementation also protects against PQ (*c*). In contrast, glucose metabolism protected against the mitochondrial complex I inhibitor MPP$^+$ while sole reliance on glutamine metabolism induced by galactose supplementation sensitized cells to MPP$^+$-induced cell death (*d*). PQ-induced AMPK signaling was shown to be dependent on iNOS (*e*). Finally, AMPK signaling activated in response to PQ or glucose deprivation exerted a protective effect against PQ (*f*), while overexpression of α-synuclein stimulated PQ toxicity (gene-environment interaction), metabolic dysfunction, and AMPK activation (*g*)

and is also regulated by glucose metabolism (Fig. 8). These findings reveal for the first time the mechanisms by which central carbon metabolism and AMPK signaling regulate gene-environment interactions involved in PD.

We previously demonstrated that PQ hijacks the PPP to use NADPH as an electron donor for its redox cycling and ROS generation (Fig. 8(a)) [30]. In this work, we now demonstrate that PQ also increases glucose uptake and that inhibition of glucose metabolism with either glucose deprivation, 2-DG, or galactose supplementation exerts a protective effect (Fig. 8(b)). Furthermore, we present evidence that the protective effect of inhibiting glucose metabolism on PQ-induced cell death is related to a decrease in the PPP and activation of AMPK. This is supported by the following observations: (1) inhibition of the PPP also reduces PQ toxicity, (2) glucose deprivation stimulates the activity of AMPK; and (3) the protective effect of glucose deprivation against PQ is hampered by inhibition of AMPK signaling. Interestingly, our results also suggest that the survival of cells under glucose deprivation might also depend on glutaminolysis and increased OXPHOS. Neurons rely on OXPHOS for ATP synthesis, while glucose metabolism seems to be primarily

directed to the generation of NADPH via the PPP to support antioxidant defenses [22]. Interestingly, neurons have been reported to use lactate and glutamine as alternative carbon sources for energy production via OXPHOS. As such, neurons can survive under glucose deprivation conditions when supplemented with lactate or glutamine [67, 68]. Galactose prompts cells to rely on glutaminolysis and OXPHOS for ATP production, and we found that galactose supplementation actually exerted a stronger protective effect against PQ toxicity compared to glucose deprivation alone [52]. Accordingly, the toxicity of the mitochondria complex I inhibitor MPP$^+$ was found to be stimulated by galactose and glucose deprivation (Fig. 8(c, d)), while PQ toxicity was also stimulated by MPP$^+$ (*data not shown*). It is important to mention that the N27 rat dopaminergic neuronal cell line is mitotically active with an intrinsic glucose metabolism that is likely to be distinct from that of post-mitotic dopaminergic neurons. Thus, the results reported here must be taken with caution. However, as mentioned above, because neurons metabolize glucose primarily to the PPP [22], our results are expected to be replicated in dopaminergic neurons. Furthermore, astrocytes, which are highly glycolytic, might actually be similarly affected by paraquat and α-

synuclein, as some studies have also reported the accumulation of α-synuclein in astrocytes in PD and dementia with Lewy bodies (DLB) [69].

We and others have reported on the protective role of autophagy against PQ-induced cell death [39, 70]. Herein, we confirmed that ULK1/ATG5-dependent autophagy exerted a protective effect against PQ toxicity. However, no additional protective effects were found when inhibiting mTOR pathway with either rapamycin or torin1, which would be expected to stimulate autophagy. While it has been reported that inhibition of glucose metabolism induces autophagy [32], we found that glucose deprivation stimulated autophagy flux, but autophagy was found impaired in PQ-treated cells cultured in glucose-free medium. Previous reports have also shown that inhibition of glucose metabolism blocks autophagy flux induced by additional stimuli [71, 72]. Thus, the protective effects of glucose deprivation seem to be largely independent of autophagy.

Glucose transporters GLUT1 (*SLC2A1*), GLUT3 (*SLC2A3*), GLUT4 (*SLC2A4*), and GLUT8 (*SLC2A8*), as well as SGLT1 and SGLT6 have been found expressed in different brain regions, but their role in neuronal function is still unclear [73]. We observed that PQ stimulated glucose transport and an increase in the levels of GLUT4 and SGLT1 glucose transporters. Furthermore, inhibition of GLUT-like transporters with STF-31 or AA (a competitive inhibitor for GLUT-like transport of glucose) also protected against PQ toxicity (Fig. 8(b)). It has also been reported that upregulation of GLUT3 protects against MPP$^+$-induced toxicity [74], which agrees with our observation that while inhibition of glucose metabolism significantly reduces PQ toxicity, it stimulates dopaminergic cell death induced by MPP$^+$. SGLT6 and GLUT8 (and probably GLUT4) seem to be the glucose transporters primarily found in the substantia nigra [75–77]. An exploratory analysis of gene-environment interactions has also suggested a possible role for the GLUT family transporter member HMIT (*SLC2A1*) in PD. Another recent study reported that Ca^{2+} overload and oxidative stress induced by PINK1 deficiency inhibit glucose transport [78]. All these findings highlight the importance of glucose transport and metabolism in dopaminergic cell death and PD.

In this work, we also found that PQ induced a selective metabolic dysfunction in the midbrain and striatum, which correlated with AMPK activation. We also found that AMPK exerts a protective effect against cell death progression (Fig. 8(f)). In particular, overexpression of a dominant-negative form of AMPKα1 sensitized cells to PQ toxicity. Accordingly, a protective role for AMPK against mitochondrial dysfunction and toxicity induced by parkin-, LRRK2-mutations, α-synuclein, and MPTP/MPP$^+$ has been previously reported [25–27]. In contrast, other reports have shown that AMPK mediates dopaminergic cell death induced by rotenone and 6-hydroxydopamine (6-OHDA) [28, 29]. As a central regulator of cellular metabolism, AMPK modulates a myriad of processes. Thus, differences between the roles of

AMPK in dopaminergic cell death induced by different PD-related insults might be related to differences in the processes regulated by AMPK or the metabolic cues involved in cell death or survival. This is evident in our results demonstrating opposite effects of glucose metabolism in dopaminergic cell death induced by MPP$^+$ or PQ (i.e., while an increase in OXPHOS and less reliance on glucose metabolism protects against PQ [Fig. 8(b, c)], increased glucose metabolism and reduced OXPHOS dependency protect against MPP$^+$). Importantly, regardless of the different metabolic requirements for PQ and MPP$^+$-induced toxicity, both insults activate AMPK (*data not shown*) suggesting that the regulatory role of AMPK on cell death progression might be complex. AMPK activation has been demonstrated to upregulate glucose transport, glycolysis, and the PPP [79–81], but inhibition of these processes reduces rather than augments PQ toxicity. Interestingly, a recent report demonstrated that AMPK inhibits glycolysis [82]. AMPK can also promote mitochondrial biogenesis and glutaminolysis [83, 84]. We found that inhibition of AMPK signaling hampers mitochondrial respiration and glycolysis, which suggests that AMPK signaling is required for cells to cope with metabolic failure induced by PQ, likely by regulating energy production, but confirmation of this hypothesis requires additional work.

AMPK activity is regulated by two inter-related processes: binding of AMP or ADP and phosphorylation [85]. An increase in the AMP (ADP)/ATP ratio is the primary trigger for AMPK phosphorylation and activation by liver kinase B1 (LKB1 or STK11) [85]. Oxidative stress has also been proposed to induce the activation of AMPK by either energy depletion, direct oxidative modification, or indirectly by LKB1 activation [63, 64, 86, 87]. NOS have been proposed to mediate oxidative stress induced by PQ, and reactive nitrogen species (RNS) are reported to activate AMPK as well [65, 66]. The iNOS inhibitor 1400W significantly reduced AMPK activity suggesting that its activation by PQ requires iNOS activity. However, we cannot discard that energy depletion and/or Ca^{2+}-dependent signaling might also be involved in AMPK activation by PQ and α-synuclein (Fig. 8(e)). Importantly, inhibition of iNOS also reduced PQ toxicity, demonstrating that iNOS has a dual role in regulating PQ-induced cell death and the activation of AMPK, which exerts a protective effect.

Importantly, while activation of AMPK by PQ was observed in dopaminergic and non-dopaminergic MEFs, in vivo AMPK activation was localized primarily to the midbrain and striatum in mice chronically treated with PQ. The reasons for these observations are unclear, but we found that AMPK activation correlated with the metabolic dysfunction induced by PQ, which was also found to be more severe in the midbrain and striatum. These results suggest that these brain regions might be more sensitive to the metabolic dysfunction induced by PQ. Previous studies have proposed that dopaminergic neurons in the substantia nigra pars compacta (SNpc) consume a significant

amount of energy during their pacemaking activity [88], for action potential generation and for the repolarization of the plasma membrane potential across the massive arborization of its unmyelinated axon [89, 90]. Together, these observations suggest that dopaminergic neurons in the substantia nigra are more sensitive to energy failure.

The mechanisms by which α-synuclein interacts with environmental exposures to induce dopaminergic cell loss are unclear. A major finding in our study is that metabolic dysfunction and AMPK activation are synergistically induced by PQ and α-synuclein and more importantly that glucose metabolism/transport and the PPP contribute to the toxic synergism of this gene-environment interaction (Fig. 8(g)). Contradictory results have been reported regarding the role of AMPK in α-synuclein aggregation and toxicity [21, 27]. PQ has been reported to accelerate the rate of formation of α-synuclein fibrils in vitro [91] and to upregulate α-synuclein expression levels and aggregation in vivo [92]. We have not observed such effects for a relatively short period of treatment with PQ (72 h) of cells overexpressing α-synuclein. While the exact mechanisms by which α-synuclein and PQ interact are unclear, our metabolomics analysis demonstrated that PQ and α-synuclein increased glucose transport/content. α-Synuclein has been reported to impair mitochondria respiration [93, 94]. PQ toxicity could be enhanced by α-synuclein-induced dysfunction in OXPHOS, which our results suggest exerts a protective effect against PQ (as evidenced by the inhibitory effect of galactose supplementation). Accordingly, similar to the effect of overexpressing dnAMPK, overexpression of α-synuclein led to a dysfunction in glycolysis and mitochondrial respiration. These results demonstrate that such metabolic dysfunction (induced by either inhibition of AMPK signaling or overexpression of α-synuclein) is the mechanisms by which PQ toxicity is enhanced.

Of note, no difference was observed between the synergism induced by the overexpression of WT α-synuclein compared to the overexpression of the PD-related mutation A53T, which is considered to be more toxic and pathogenic [95, 96]. Interestingly, we found that murine (rat or mouse) α-synuclein already has an Ala at amino acid position 53. We were unable to find any previous reference to this observation in the literature, but it might suggest that mice have intrinsic mechanisms protecting against the deleterious effects of A53T α-synuclein (or multiplications)and may explain why some transgenic mouse overexpressing A53T α-synuclein (or other α-synuclein variants) show no major degeneration of dopaminergic cells [97, 98].

Overall our results demonstrate for the first time that glucose metabolism and AMPK contribute to dopaminergic cell death induced by PQ and α-synuclein interactions. These results reveal the importance of central carbon metabolism and metabolic dysfunction/signaling in dopaminergic cell death induced by gene-environment interactions.

References

1. Niccoli T, Partridge L (2012) Ageing as a risk factor for disease. Curr Biol 22(17):R741–52

2. Cannon JR, Greenamyre JT (2013) Gene-environment interactions in Parkinson's disease: specific evidence in humans and mammalian models. Neurobiol Dis 57:38–46

3. Klein C, Westenberger A (2012) Genetics of Parkinson's disease. Cold Spring Harb Perspect Med 2(1):a008888

4. Polymeropoulos MH, Lavedan C, Leroy E, Ide SE, Dehejia A, Dutra A et al (1997) Mutation in the alpha-synuclein gene identified in families with Parkinson's disease. Science 276(5321):2045–7

5. Stefanis L (2012) Alpha-synuclein in Parkinson's disease. Cold Spring Harb Perspect Med 2(2):a009399

6. Singleton AB, Farrer M, Johnson J, Singleton A, Hague S, Kachergus J et al (2003) Alpha-synuclein locus triplication causes Parkinson's disease. Science 302(5646):841

7. Chartier-Harlin MC, Kachergus J, Roumier C, Mouroux V, Douay X, Lincoln S et al (2004) Alpha-synuclein locus duplication as a cause of familial Parkinson's disease. Lancet 364(9440):1167–9

8. Ross OA, Braithwaite AT, Skipper LM, Kachergus J, Hulihan MM, Middleton FA et al (2008) Genomic investigation of alpha-synuclein multiplication and parkinsonism. Ann Neurol 63(6):743–50

9. Tanner CM, Kamel F, Ross GW, Hoppin JA, Goldman SM, Korell M et al (2011) Rotenone, paraquat, and Parkinson's disease. Environ Health Perspect 119(6):866–72

10. Rodriguez-Rocha H, Garcia-Garcia A, Pickett C, Li S, Jones J, Chen H et al (2013) Compartmentalized oxidative stress in dopaminergic cell death induced by pesticides and complex I inhibitors: distinct roles of superoxide anion and superoxide dismutases. Free Radic Biol Med 61C:370–383

11. Franco R, Li S, Rodriguez-Rocha H, Burns M, Panayiotidis MI (2010) Molecular mechanisms of pesticide-induced neurotoxicity: relevance to Parkinson's disease. Chem Biol Interact 188(2):289–300

12. Ryan SD, Dolatabadi N, Chan SF, Zhang X, Akhtar MW, Parker J et al (2013) Isogenic human iPSC Parkinson's model shows nitrosative stress-induced dysfunction in MEF2-PGC1alpha transcription. Cell 155(6):1351–64

13. Norris EH, Uryu K, Leight S, Giasson BI, Trojanowski JQ, Lee VM (2007) Pesticide exposure exacerbates alpha-synucleinopathy in an A53T transgenic mouse model. Am J Pathol 170(2):658–66

14. Peng J, Oo ML, Andersen JK (2010) Synergistic effects of environmental risk factors and gene mutations in Parkinson's disease accelerate age-related neurodegeneration. J Neurochem 115(6):1363–73

15. Perier C, Vila M (2012) Mitochondrial biology and Parkinson's disease. Cold Spring Harb Perspect Med 2(2):a009332

16. Gibson GE, Kingsbury AE, Xu H, Lindsay JG, Daniel S, Foster OJ et al (2003) Deficits in a tricarboxylic acid cycle enzyme in brains from patients with Parkinson's disease. Neurochem Int 43(2):129–35

17. Yin F, Boveris A, Cadenas E (2014) Mitochondrial energy metabolism and redox signaling in brain aging and neurodegeneration. Antioxid Redox Signal 20(2):353–71

18. Palombo E, Porrino LJ, Bankiewicz KS, Crane AM, Sokoloff L, Kopin IJ (1990) Local cerebral glucose utilization in monkeys with hemiparkinsonism induced by intracarotid infusion of the neurotoxin MPTP. J Neurosci 10(3):860–9

19. Eberling JL, Richardson BC, Reed BR, Wolfe N, Jagust WJ (1994) Cortical glucose metabolism in Parkinson's disease without dementia. Neurobiol Aging 15(3):329–35

20. Henchcliffe C, Shungu DC, Mao X, Huang C, Nirenberg MJ, Jenkins BG et al (2008) Multinuclear magnetic resonance spectroscopy for in vivo assessment of mitochondrial dysfunction in Parkinson's disease. Ann N Y Acad Sci 1147:206–20

21. Jiang P, Gan M, Ebrahim AS, Castanedes-Casey M, Dickson DW, Yen SH (2013) Adenosine monophosphate-activated protein kinase overactivation leads to accumulation of alpha-synuclein oligomers and decrease of neurites. Neurobiol Aging 34(5):1504–15

22. Herrero-Mendez A, Almeida A, Fernandez E, Maestre C, Moncada S, Bolanos JP (2009) The bioenergetic and antioxidant status of neurons is controlled by continuous degradation of a key glycolytic enzyme by APC/C-Cdh1. Nat Cell Biol 11(6):747–52

23. Dunn L, Allen GF, Mamais A, Ling H, Li A, Duberley KE et al (2014) Dysregulation of glucose metabolism is an early event in sporadic Parkinson's disease. Neurobiol Aging 35(5):1111–5

24. Cardaci S, Filomeni G, Ciriolo MR (2012) Redox implications of AMPK-mediated signal transduction beyond energetic clues. J Cell Sci 125(Pt 9):2115–25

25. Ng CH, Guan MS, Koh C, Ouyang X, Yu F, Tan EK et al (2012) AMP kinase activation mitigates dopaminergic dysfunction and mitochondrial abnormalities in Drosophila models of Parkinson's disease. J Neurosci 32(41):14311–7

26. Choi JS, Park C, Jeong JW (2010) AMP-activated protein kinase is activated in Parkinson's disease models mediated by 1-methyl-4-phenyl-1,2,3,6-tetrahydropyridine. Biochem Biophys Res Commun 391(1):147–51

27. Dulovic M, Jovanovic M, Xilouri M, Stefanis L, Harhaji-Trajkovic L, Kravic-Stevovic T et al (2014) The protective role of AMP-activated protein kinase in alpha-synuclein neurotoxicity in vitro. Neurobiol Dis 63:1–11

28. Xu Y, Liu C, Chen S, Ye Y, Guo M, Ren Q et al (2014) Activation of AMPK and inactivation of Akt result in suppression of mTOR-mediated S6K1 and 4E-BP1 pathways leading to neuronal cell death in in vitro models of Parkinson's disease. Cell Signal 26(8):1680–9

29. Kim TW, Cho HM, Choi SY, Suguira Y, Hayasaka T, Setou M et al (2013) (ADP-ribose) polymerase 1 and AMP-activated protein kinase mediate progressive dopaminergic neuronal degeneration in a mouse model of Parkinson's disease. Cell Death Dis 4:e919

30. Lei S, Zavala-Flores L, Garcia-Garcia A, Nandakumar R, Huang Y, Madayiputhiya N et al (2014) Alterations in energy/redox metabolism induced by mitochondrial and environmental toxins: a specific role for glucose-6-phosphate-dehydrogenase and the pentose phosphate pathway in paraquat toxicity. ACS Chem Biol

31. Prasad KN, Carvalho E, Kentroti S, Edwards-Prasad J, Freed C, Vernadakis A (1994) Establishment and characterization of immortalized clonal cell lines from fetal rat mesencephalic tissue. In Vitro Cell Dev Biol Anim 30A(9):596–603

32. Kim J, Kundu M, Viollet B, Guan KL (2011) AMPK and mTOR regulate autophagy through direct phosphorylation of Ulk1. Nat Cell Biol 13(2):132–41

33. Liu F, Hindupur J, Nguyen JL, Ruf KJ, Zhu J, Schieler JL et al (2008) Methionine sulfoxide reductase A protects dopaminergic cells from Parkinson's disease-related insults. Free Radic Biol Med 45(3):242–55

34. Yang L, Li P, Fu S, Calay ES, Hotamisligil GS (2010) Defective hepatic autophagy in obesity promotes ER stress and causes insulin resistance. Cell Metab 11(6):467–78

35. Zimmerman MC, Lazartigues E, Lang JA, Sinnayah P, Ahmad IM, Spitz DR et al (2002) Superoxide mediates the actions of angiotensin II in the central nervous system. Circ Res 91(11):1038–45

36. Woods A, Azzout-Marniche D, Foretz M, Stein SC, Lemarchand P, Ferre P et al (2000) Characterization of the role of AMP-activated protein kinase in the regulation of glucose-activated gene expression using constitutively active and dominant negative forms of the kinase. Mol Cell Biol 20(18):6704–11

37. Barde I, Salmon P, Trono D (2010) Production and titration of lentiviral vectors. Curr Protoc Neurosci; Chapter 4: Unit 4 21

38. Rodriguez-Rocha H, Garcia-Garcia A, Zavala-Flores L, Li S, Madayiputhiya N, Franco R (2012) Glutaredoxin 1 protects dopaminergic cells by increased protein glutathionylation in experimental Parkinson's disease. Antioxid Redox Signal

39. Garcia-Garcia A, Anandhan A, Burns M, Chen H, Zhou Y, Franco R (2013) Impairment of Atg5-dependent autophagic flux promotes paraquat- and MPP(+)-induced apoptosis but not rotenone or 6-hydroxydopamine toxicity. Toxicol Sci 136(1):166–82

40. Anandhan A, Rodriguez-Rocha H, Bohovych I, Griggs AM, Zavala-Flores L, Reyes-Reyes EM et al (2014) Overexpression of alpha-synuclein at non-toxic levels increases dopaminergic cell death induced by copper exposure via modulation of protein degradation pathways. Neurobiol Dis

41. Navarro-Yepes J, Anandhan A, Bradley E, Bohovych I, Yarabe B, de Jong A et al (2015) Inhibition of protein ubiquitination by paraquat and 1-methyl-4-phenylpyridinium impairs ubiquitin-dependent protein degradation pathways. Mol Neurobiol

42. Teslaa T, Teitell MA (2014) Techniques to monitor glycolysis. Methods Enzymol 542:91–114

43. Brand MD, Nicholls DG (2011) Assessing mitochondrial dysfunction in cells. Biochem J 435(2):297–312

44. Chaika NV, Gebregiworgis T, Lewallen ME, Purohit V, Radhakrishnan P, Liu X et al (2012) MUC1 mucin stabilizes and activates hypoxia-inducible factor 1 alpha to regulate metabolism in pancreatic cancer. Proc Natl Acad Sci U S A 109(34):13787–92

45. Worley B, Powers R (2014) MVAPACK: a complete data handling package for NMR metabolomics. ACS Chem Biol 9(5):1138–44

46. Marshall DD, Lei S, Worley B, Huang Y, Garcia-Garcia A, Franco R et al (2015) Combining DI-ESI-MS and NMR datasets for metabolic profiling. Metabolomics 11(2):391–402

47. Worley B, Halouska S, Powers R (2013) Utilities for quantifying separation in PCA/PLS-DA scores plots. Anal Biochem 433(2):102–4

48. Werth MT, Halouska S, Shortridge MD, Zhang B, Powers R (2010) Analysis of metabolomic PCA data using tree diagrams. Anal Biochem 399(1):58–63

49. Eriksson L, Trygg J, Wold S (2008) CV-ANOVA for significance testing of PLS and OPLS (R) models. J Chemometr 22(11–12):594–600

50. Shao J (1993) Linear-model selection by cross-validation. J Am Stat Assoc 88(422):486–494

51. Marroquin LD, Hynes J, Dykens JA, Jamieson JD, Will Y (2007) Circumventing the Crabtree effect: replacing media glucose with galactose increases susceptibility of HepG2 cells to mitochondrial toxicants. Toxicol Sci 97(2):539–47

52. Reitzer LJ, Wice BM, Kennell D (1979) Evidence that glutamine, not sugar, is the major energy source for cultured HeLa cells. J Biol Chem 254(8):2669–76

53. Klionsky DJ, Abdalla FC, Abeliovich H, Abraham RT, Acevedo-Arozena A, Adeli K et al (2012) Guidelines for the use and interpretation of assays for monitoring autophagy. Autophagy 8(4):445–544

54. Kim YC, Guan KL (2015) mTOR: a pharmacologic target for autophagy regulation. J Clin Invest 125(1):25–32

55. Chiang GG, Abraham RT (2005) Phosphorylation of mammalian target of rapamycin (mTOR) at Ser-2448 is mediated by p70S6 kinase. J Biol Chem 280(27):25485–90

56. Russell RC, Tian Y, Yuan H, Park HW, Chang YY, Kim J et al (2013) ULK1 induces autophagy by phosphorylating Beclin-1 and activating VPS34 lipid kinase. Nat Cell Biol 15(7):741–50

57. Egan DF, Shackelford DB, Mihaylova MM, Gelino S, Kohnz RA, Mair W et al (2011) Phosphorylation of ULK1 (hATG1) by AMP-activated protein kinase connects energy sensing to mitophagy. Science 331(6016):456–61

58. Rumsey SC, Daruwala R, Al-Hasani H, Zarnowski MJ, Simpson IA, Levine M (2000) Dehydroascorbic acid transport by GLUT4 in Xenopus oocytes and isolated rat adipocytes. J Biol Chem 275(36): 28246–53

59. Cantu D, Fulton RE, Drechsel DA, Patel M (2011) Mitochondrial aconitase knockdown attenuates paraquat-induced dopaminergic cell death via decreased cellular metabolism and release of iron and H(2)O(2). J Neurochem 118(1):79–92

60. Viollet B, Horman S, Leclerc J, Lantier L, Foretz M, Billaud M et al (2010) AMPK inhibition in health and disease. Crit Rev Biochem Mol Biol 45(4):276–95

61. Laderoute KR, Amin K, Calaoagan JM, Knapp M, Le T, Orduna J et al (2006) 5′-AMP-activated protein kinase (AMPK) is induced by low-oxygen and glucose deprivation conditions found in solid-tumor microenvironments. Mol Cell Biol 26(14):5336–47

62. O'Neill HM, Maarbjerg SJ, Crane JD, Jeppesen J, Jorgensen SB, Schertzer JD et al (2011) AMP-activated protein kinase (AMPK) beta1beta2 muscle null mice reveal an essential role for AMPK in maintaining mitochondrial content and glucose uptake during exercise. Proc Natl Acad Sci U S A 108(38):16092–7

63. Zmijewski JW, Banerjee S, Bae H, Friggeri A, Lazarowski ER, Abraham E (2010) Exposure to hydrogen peroxide induces oxidation and activation of AMP-activated protein kinase. J Biol Chem 285(43):33154–64

64. Auciello FR, Ross FA, Ikematsu N, Hardie DG (2014) Oxidative stress activates AMPK in cultured cells primarily by increasing cellular AMP and/or ADP. FEBS Lett 588(18):3361–6

65. Day BJ, Patel M, Calavetta L, Chang LY, Stamler JS (1999) A mechanism of paraquat toxicity involving nitric oxide synthase. Proc Natl Acad Sci U S A 96(22):12760–5

66. Ortiz-Ortiz MA, Moran JM, Gonzalez-Polo RA, Niso-Santano M, Soler G, Bravo-San Pedro JM et al (2009) Nitric oxide-mediated toxicity in paraquat-exposed SH-SY5Y cells: a protective role of 7-nitroindazole. Neurotox Res 16(2):160–73

67. Schurr A, West CA, Rigor BM (1988) Lactate-supported synaptic function in the rat hippocampal slice preparation. Science 240(4857):1326–8

68. Monyer H, Choi DW (1990) Glucose deprivation neuronal injury in vitro is modified by withdrawal of extracellular glutamine. J Cereb Blood Flow Metab 10(3):337–42

69. Bruck D, Wenning GK, Stefanova N, Fellner L (2016) Glia and alpha-synuclein in neurodegeneration: a complex interaction. Neurobiol Dis 85:262–74

70. Wills J, Credle J, Oaks AW, Duka V, Lee JH, Jones J et al (2012) Paraquat, but not maneb, induces synucleinopathy and tauopathy in striata of mice through inhibition of proteasomal and autophagic pathways. PLoS One 7(1), e30745

71. Ramirez-Peinado S, Leon-Annicchiarico CL, Galindo-Moreno J, Iurlaro R, Caro-Maldonado A, Prehn JH et al (2013) Glucose-starved cells do not engage in prosurvival autophagy. J Biol Chem 288(42):30387–98

72. Dodson M, Liang Q, Johnson MS, Redmann M, Fineberg N, Darley-Usmar VM et al (2013) Inhibition of glycolysis attenuates 4-hydroxynonenal-dependent autophagy and exacerbates apoptosis in differentiated SH-SY5Y neuroblastoma cells. Autophagy 9(12): 1996–2008

73. Shah K, Desilva S, Abbruscato T (2012) The role of glucose transporters in brain disease: diabetes and Alzheimer's disease. Int J Mol Sci 13(10):12629–55

74. Chaudhuri AD, Kabaria S, Choi DC, Mouradian MM, Junn E (2015) MicroRNA-7 promotes glycolysis to protect against 1-methyl-4-phenylpyridinium-induced cell death. J Biol Chem 290(19):12425–34

75. Sankar R, Thamotharan S, Shin D, Moley KH, Devaskar SU (2002) Insulin-responsive glucose transporters-GLUT8 and GLUT4 are expressed in the developing mammalian brain. Brain Res Mol Brain Res 107(2):157–65

76. Chen J, Williams S, Ho S, Loraine H, Hagan D, Whaley JM et al (2010) Quantitative PCR tissue expression profiling of the human SGLT2 gene and related family members. Diab Ther 1(2):57–92

77. El Messari S, Ait-Ikhlef A, Ambroise DH, Penicaud L, Arluison M (2002) Expression of insulin-responsive glucose transporter GLUT4 mRNA in the rat brain and spinal cord: an in situ hybridization study. J Chem Neuroanat 24(4):225–42

78. Gandhi S, Wood-Kaczmar A, Yao Z, Plun-Favreau H, Deas E, Klupsch K et al (2009) PINK1-associated Parkinson's disease is caused by neuronal vulnerability to calcium-induced cell death. Mol Cell 33(5):627–38

79. Wu SB, Wei YH (2012) AMPK-mediated increase of glycolysis as an adaptive response to oxidative stress in human cells: implication of the cell survival in mitochondrial diseases. Biochim Biophys Acta 1822(2):233–47

80. Kurth-Kraczek EJ, Hirshman MF, Goodyear LJ, Winder WW (1999) 5′ AMP-activated protein kinase activation causes GLUT4 translocation in skeletal muscle. Diabetes 48(8):1667–71

81. Jeon SM, Chandel NS, Hay N (2012) AMPK regulates NADPH homeostasis to promote tumour cell survival during energy stress. Nature 485(7400):661–5

82. Faubert B, Boily G, Izreig S, Griss T, Samborska B, Dong Z et al (2013) AMPK is a negative regulator of the Warburg effect and suppresses tumor growth in vivo. Cell Metab 17(1):113–24

83. Reznick RM, Shulman GI (2006) The role of AMP-activated protein kinase in mitochondrial biogenesis. J Physiol 574(Pt 1):33–9

84. Nieminen AI, Eskelinen VM, Haikala HM, Tervonen TA, Yan Y, Partanen JI et al (2013) Myc-induced AMPK-phospho p53 pathway activates Bak to sensitize mitochondrial apoptosis. Proc Natl Acad Sci U S A 110(20):E1839–48

85. Hardie DG (2014) AMP-activated protein kinase: maintaining energy homeostasis at the cellular and whole-body levels. Annu Rev Nutr 34:31–55

86. Shaw RJ, Kosmatka M, Bardeesy N, Hurley RL, Witters LA, Depinho RA et al (2004) The tumor suppressor LKB1 kinase directly activates AMP-activated kinase and regulates apoptosis in response to energy stress. Proc Natl Acad Sci U S A 101(10):3329–35

87. Shao D, Oka S, Liu T, Zhai P, Ago T, Sciarretta S et al (2014) A redox-dependent mechanism for regulation of AMPK activation by Thioredoxin1 during energy starvation. Cell Metab 19(2):232–45

88. Guzman JN, Sanchez-Padilla J, Wokosin D, Kondapalli J, Ilijic E, Schumacker PT et al (2010) Oxidant stress evoked by pacemaking in dopaminergic neurons is attenuated by DJ-1. Nature 468(7324): 696–700

89. Pissadaki EK, Bolam JP (2013) The energy cost of action potential propagation in dopamine neurons: clues to susceptibility in Parkinson's disease. Front Comput Neurosci 7:13

90. Matsuda W, Furuta T, Nakamura KC, Hioki H, Fujiyama F, Arai R et al (2009) Single nigrostriatal dopaminergic neurons form widely spread and highly dense axonal arborizations in the neostriatum. J Neurosci 29(2):444–53

91. Uversky VN, Li J, Fink AL (2001) Pesticides directly accelerate the rate of alpha-synuclein fibril formation: a possible factor in Parkinson's disease. FEBS Lett 500(3):105–8

92. Manning-Bog AB, McCormack AL, Li J, Uversky VN, Fink AL, Di Monte DA (2002) The herbicide paraquat causes up-regulation and aggregation of alpha-synuclein in mice: paraquat and alpha-synuclein. J Biol Chem 277(3):1641–4

93. Subramaniam SR, Vergnes L, Franich NR, Reue K, Chesselet MF (2014) Region specific mitochondrial impairment in mice with widespread overexpression of alpha-synuclein. Neurobiol Dis 70: 204–13

94. Devi L, Raghavendran V, Prabhu BM, Avadhani NG, Anandatheerthavarada HK (2008) Mitochondrial import and accumulation of alpha-synuclein impair complex I in human dopaminergic neuronal cultures and Parkinson disease brain. J Biol Chem 283(14):9089–100

95. Conway KA, Lee SJ, Rochet JC, Ding TT, Williamson RE, Lansbury PT Jr (2000) Acceleration of oligomerization, not fibrillization, is a shared property of both alpha-synuclein mutations linked to early-onset Parkinson's disease: implications for pathogenesis and therapy. Proc Natl Acad Sci U S A 97(2):571–6

96. Dettmer U, Newman AJ, Soldner F, Luth ES, Kim NC, von Saucken VE et al (2015) Parkinson-causing alpha-synuclein missense mutations shift native tetramers to monomers as a mechanism for disease initiation. Nat Commun 6:7314

97. Martin LJ, Pan Y, Price AC, Sterling W, Copeland NG, Jenkins NA et al (2006) Parkinson's disease alpha-synuclein transgenic mice develop neuronal mitochondrial degeneration and cell death. J Neurosci 26(1):41–50

98. Masliah E, Rockenstein E, Veinbergs I, Mallory M, Hashimoto M, Takeda A et al (2000) Dopaminergic loss and inclusion body formation in alpha-synuclein mice: implications for neurodegenerative disorders. Science 287(5456):1265–9